electronics

Article

A Flexible Lightweight Triboelectric Nanogenerator for Protector and Scoring System in Taekwondo Competition Monitoring

Fengxin Sun [1], Yongsheng Zhu [1], Changjun Jia [1], Bowen Ouyang [1], Tianming Zhao [2], Caixia Li [1], Ning Ba [3], Xinxing Li [4], Song Chen [1,*], Tongtong Che [3,5,*] and Yupeng Mao [1,*]

1 Physical Education Department, Northeastern University, Shenyang 110819, China; 2171435@stu.neu.edu.cn (F.S.); 2001276@stu.neu.edu.cn (Y.Z.); 2071367@stu.neu.edu.cn (C.J.); oybw945@126.com (B.O.); 2101264@stu.neu.edu.cn (C.L.)
2 College of Sciences, Northeastern University, Shenyang 110819, China; zhaotm@stumail.neu.edu.cn
3 Department of Sports Science and Physical Education, Tsinghua University, Beijing 100084, China; justbill@mail.tsinghua.edu.cn
4 Department of Physical Education, Seoul National University, Seoul 08826, Korea; shinsunglee2021@snu.ac.kr
5 Capital University of Physical Education and Sport, Beijing 100191, China
* Correspondence: chensong@pe.neu.edu.cn (S.C.); chetongtong2018@cupes.edu.cn (T.C.); maoyupeng@pe.neu.edu.cn (Y.M.)

Abstract: Nowadays, the applications of the triboelectric nanogenerator in sensing and monitoring sports experience a blooming prosperity. Here, we report a flexible and lightweight triboelectric nanogenerator (FL-TENG) made of hydrogel electrodes, polytetrafluoroethylene (PTFE), PDMS, and polyurethane (PU). Based on the triboelectric effect, the FL-TENG can work as a self-powered sensor attaching to taekwondo protective gear, which can be used to monitor athletes' competition performance and improve the fairness of the competition. In addition, the FL-TENG can drive micro-wireless devices for wireless transmitting sports data during the competition in real time. This kind of sustainable green self-powered sensor provides a new path for the field of sports competition monitoring.

Keywords: self-powered; sustainable energy storage; human motion monitoring; portable sensor; triboelectric nanogenerator

Citation: Sun, F.; Zhu, Y.; Jia, C.; Ouyang, B.; Zhao, T.; Li, C.; Ba, N.; Li, X.; Chen, S.; Che, T.; et al. A Flexible Lightweight Triboelectric Nanogenerator for Protector and Scoring System in Taekwondo Competition Monitoring. *Electronics* **2022**, *11*, 1306. https://doi.org/10.3390/electronics11091306

Academic Editor: Antonio Di Bartolomeo

Received: 30 March 2022
Accepted: 17 April 2022
Published: 20 April 2022

1. Introduction

With the rapid development of artificial intelligence, big data, intelligence, automation, etc., [1–8], all of these have affected all aspects of people's activities, such as smart homes, unmanned supermarkets, unmanned buses, earthquake warnings, environmental quality monitoring, and so on [9–18]. Similarly, there are big changes in the field of sports as they enter the era of digitalization and intelligence, such as the real-time monitoring of athletes' heart rate, blood pressure and blood lactate, virtual reality training, and body composition testing [19–23], all of which help athletes in their daily training and competitive ability. Recently, the issue of fairness and impartiality of refereeing in taekwondo competitions has aroused heated debates, and it is common for athletes and coaches to complain about the lack of reasonableness of refereeing decisions during traditional competitive taekwondo competitions. The use of electronic chips in inductive electronic protective gear in taekwondo competitions has greatly improved the brilliance, achievements, and fairness of competitive taekwondo competitions [24]. However, the use of electronic protective gear also exposes the problems of short device life, heavy weight, long debugging time, and low sensitivity. In order to better develop taekwondo, it is necessary to develop a sustainable, time-saving, lightweight, and sensitive sensing device.

In recent years, most of the numerous studies about sensors still use traditional batteries for energy storage and power supply. Although battery-driven sensor devices are widely used in many fields, in the field of wearable sensing devices, especially for motion monitoring, battery-driven sensors have certain limitations due to their size and weight. Recently reported research on thermoelectric and triboelectric technologies provides more options to address self-powered sensing, such as thermoelectric devices for personal thermal management, which automatically regulate human body temperature while also collecting waste heat generated by the human body for energy storage [25–27], and triboelectric technologies to convert and store energy from natural wind, water, and motion mechanical energy. Thermoelectricity and frictional electricity as advanced self-powered sensing technologies demonstrate their respective advantages in different fields. Since Professor Zhonglin Wang invented the triboelectric nanogenerator in 2012 [28], the triboelectric nanogenerator has been widely used in the collection of environmental energy sources [29–35], motion information monitoring [36–39], and medical monitoring [40–44] because of their demonstrated excellent working performance, sustainability, simple structure, diverse materials, and green environment. It has been.demonstrated that a soft-contact spherical triboelectric nanogenerator, which increases the output charge by increasing the contact area, can be used to obtain blue energy from ocean waves [45]. Based on a simple and effective strategy, natural wood can be transformed into triboelectric materials with excellent mechanical properties, which can be used for self-powered sensing in a big data analysis of motion [46]. The triboelectric nanogenerator with an integrated facemask can be used for respiratory monitoring [47]. Triboelectric nanogenerators can be used as both energy harvesting and signal transmission devices, and they are characterized by small size, lightweight, stable operating performance, and high sensitivity. This provides a new idea to solve the defective problem of electronic protective gear in competitive taekwondo.

In this study, we report a triboelectric nanogenerator (FL-TENG) with transparent polytetrafluoroethylene (PTFE) film and transparent polyurethane (PU) film as the friction layers, polydimethylsiloxane (PDMS) as the support layer, and hydrogel as the electrode. It can be attached to the inner layer or surface of the taekwondo protective gear, and through the triboelectric effect, it converts the mechanical energy of strikes into electrical energy, which can drive the body and transmit signals at the same time, and also monitor the position and strength of the player's strike position. In addition, as the material of taekwondo protective gear is polyurethane (PU), the triboelectric device can also directly establish a friction layer with the taekwondo protective gear, reducing the use of materials and reducing the weight of the device. Hydrogel, as a flexible electrode, is low in production cost, simple, and stretchable. The stretchable property of the hydrogel ensures that the electrodes will not be broken under the violent impact, thus further improving the device life and stability of the device. Therefore, the combination of this device and taekwondo protective gear makes up for the short life span, heavyweight, long debugging time, and low sensitivity of electronic protective gear, and at the same time, this device can help the referee to judge whether the attack is effective, whether the action is foul, assist the referee to score, help the coach to analyze the athletes' strike point distribution, attack rhythm, and effective scoring action, to comply with the principle of competitive needs and scientific arrangement of the athletes' training. In general, the developed work and related technology of the FL-TENG solves the problem of defects in the existing taekwondo electronic protective gear. The combination of FL-TENG and wireless transmission systems provides a boost for sports competition monitoring and training and even provides a reference for the development of intelligence in the field of infinite sport big data and in the field of human–computer interaction.

2. Experiment

2.1. Materials

Polyurethane (PU) film was purchased from Dongguan Jinda Plastic Insulation Material Shop (Dongguan, China). Transparent PTFE was purchased from Taizhou Huafu

Plastic Industry Co., Ltd. (Taizhou, China). *N*, *N*-dimethylformamide (DMF), deionized water, acrylamide (AM), lithium chloride (LiCl), *N*0, *N*0-methylene diacrylamide (MBA), ammonium persulfate (APS), and *N*0, *N*0, *N*0, *N*0-tetramethylethylenediamine (TMLD) were purchased from Jintong Loctite (Beijing, China). Dow Corning DC184 was purchased from Xinheng Trading Co., Ltd. (Tianjin, China).

2.2. Production of FL-TENG

PDMS support layer fabrication: First, PDMS solution and curing agent were mixed in a 10:1 weight ratio and stirred for 2 min to make them well mixed. Next, the mixed solution was shaken for 10 min using a water bath ultrasonic oscillator to remove air bubbles. Finally, after shaking for 10 min, we poured it on the mold and dried it in a blast drying oven at 80 °C for 15 min to get the PDMS support layer.

Preparation of hydrogels: AM as monomer, MBA as cross-linker, APS as initiator, and TMEDA as the catalyst. First, 35 mL of pure water and 5 mL of deionized water were weighed and mixed, and 12 g of acrylamide powder and 14 g of lithium chloride particles were added to them and stirred using a magnetic stirrer at 800 rpm to obtain 4.23 mol/L and 8.24 mol/L of mixed AM and LiCl solutions. Next, 0.04 mol/L APS and 0.03 mol/L MBA were added to the mixed solution simultaneously to obtain the pre-solution. Finally, the pre-solution was poured on the mold, and a drop of TMEDA was added to accelerate the association of the hydrogels to obtain PAAM-LiCl hydrogels.

Complete fabrication of the device: Firstly, PU film and PTFE film of the same size were cut according to the size of the PDMS support layer, respectively. Secondly, the hydrogel electrodes were cut according to the size of PU and PTFE films, and the hydrogel electrodes were closely laminated with PU and PTFE films to form the two friction layers of TENG. Finally, the PTFE film is used as the electronegative layer, the flexible PDMS is used as the middle support layer to facilitate the contact and separation of the two friction layers, and the PU film is used as the electropositive layer. The three layers are stacked sequentially and are fixed at both ends with tape to form the complete device.

2.3. Characterization and Measurement

The FL-TENG is fixed to a stepper motor to simulate a taekwondo competition strike. The performance of the FL-TENG was tested using different amplitudes and frequencies. The sensing signals were generated by the FL-TENG and acquired by an oscilloscope (Shenzhen sto1102c, Shenzhen, China). The morphology and structure of the PU film were performed by an optical microscope (sunshine instrumentation co., SDPTOP-CX 40 m, Ningbo, China). The cross-sectional morphology and structure of the device were performed by a scanning electron microscope (HITACHI S-4800).

2.4. Data Acquisition System

The performance of FL-TENG plays a decisive role in the feasibility of the application of self-powered sensing. To test the electrical performance of FL-TENG, we designed a data acquisition system. The data acquisition system consists of two parts; one is an electrical signal generation system driven by a stepper motor. FL-TENG is attached to a fixed baffle, and by setting the stepping frequency and stepping distance of the stepper motor the frequency and angle change of the FL-TENG contact separation is controlled. FL-TENG collects and converts the mechanical energy generated by the stepper motor into electrical energy. The second part is an oscilloscope-based electrical signal acquisition system, which collects the electrical energy converted by FL-TENG in the form of electrical signals and displays them in the form of waveforms. In this study, the stepper motor is only used to test the electrical performance of the FL-TENG. In the real application, the FL-TENG is attached to the human body to collect biomechanical energy, and the electrical signal is captured by the oscilloscope (as shown in Videos S3–S7). To further adapt to the needs of practical applications, we designed a wireless data transmission system, which consists of a signal transmitting module and a signal receiving module. The signal transmitting module

is connected to the FL-TENG to transmit the electrical signal wirelessly to the receiving module, which is connected to a computer and can perform data acquisition and waveform display (as shown in Video S8).

3. Results and Discussion

In this study, we applied FL-TENG to taekwondo competition monitoring. As shown in Figure 1a, FL-TENG is attached to the back of taekwondo protective gear, allowing for energy harvesting and wireless transmission, as well as real-time monitoring of taekwondo competitions and daily training. As shown in Figure 1b, FL-TENG can be applied to various sports monitoring, and the biomechanical energy is collected by FL-TENG and converted into electrical energy for motion data transmission, which makes the motion monitoring data intelligent. Figure 1c shows the fabrication process of FL-TENG. First, acrylamide, lithium chloride, ammonium persulfate, and NN-methylene bisacrylamide were mixed in a certain ratio and catalyzed with TMEDA to obtain the hydrogel electrode. Then, the PDMS solution and curing agent were mixed in a weight ratio of 10:1, the air bubbles were removed, and then poured into the mold. Next, they were dried at 80 °C to get the support layer. Finally, the complete device is obtained by stacking the upper polyurethane (PU) film, the middle PDMS support layer, the lower polytetrafluoroethylene (PTFE) film, and the hydrogel electrode distributed on the upper and lower surfaces. Figure 1d shows an optical microscope image of the polyurethane film. The scanning electron microscope images of the cross-sections of the PU and PTFE layers are shown in Figure 1e–f, respectively, through which it can be observed that there is no gap between the hydrogel electrode and the two friction layers in a tight fit. Figure 1g demonstrates the soft and bendable nature of FL-TENG, and the flexible sensing device makes it safer and more comfortable to wear protective gear.

The working mechanism of FL-TENG is shown in Figure 2a, which shows the single electrical output process of FL-TENG. In this figure, the polyurethane (PU) film is used as the top dielectric friction layer, polytetrafluoroethylene (PTFE) is used as the bottom dielectric friction layer, PDMS is used as the middle support layer to facilitate the contact and separation between the two friction layers of PU film and PTFE film, and the hydrogel is used as the conductive electrode. We consider the material selection criteria from three levels. The first level, the electrical output performance that the two friction layer materials can produce, and FL-TENG as a self-powered sensor for competition monitoring, has high requirements for the size, stability, and sensitivity of the output voltage. In the second level, the selected material should be light and flexible, because as a device that is attached to the human body for competition monitoring, its safety and comfort must be the key consideration. In the third level, the selected material should have the ability to resist blows and not be easy to break, in order to maintain a long service life. Combining the above three levels, the PTFE film has very good electronegativity, the PU film has very good electronegativity [48], and in this study, the combination of these two materials can produce an output of up to 514 volts, and keep a sensitive and stable output for a long time. The hydrogel electrode and PDMS support layer increase the lifetime of the device while ensuring that the device has flexible and stretchable properties. Initially, FL-TENG is not subjected to external forces, and the top and bottom dielectric friction layers are separated; this demonstrates an electrically neutral without a charge and electrical output (state I). When an external force is applied to the FL-TENG, the FL-TENG is deformed, resulting in a complete contact between the polyurethane (PU) friction layer and the polytetrafluoroethylene (PTFE) friction layer, and due to the frictional electric effect, it produces frictional electricity. The polyurethane (PU) layer tends to lose electrons and the polytetrafluoroethylene (PTFE) layer tends to gain electrons easily, and electrons are transferred from the surface of the polyurethane (PU) layer to the polytetrafluoroethylene (PTFE) layer (state II). When the applied external force disappears gradually, the upper friction layer and the lower friction layers are separated, and the charge separation on the surface of the friction layer generates a potential difference, which drives the charge

transfer from the electrode with the PTFE layer to the electrode with PU layer (state III). When the applied external force disappears completely, the charge transfer ends and the electron flow stops (state IV). When the FL-TENG is compressed by the force again, the upper and lower friction layers approach each other to produce a reverse internal electric field, and electrons are transferred from the electrode with the polyurethane (PU) layer to the electrode with the polytetrafluoroethylene (PTFE) layer (state V). A cycle is completed when the upper and bottom friction layers are in full contact. Afterward, the FL-TENG is compressed and released to start a new cycle. Corresponding simulations of potential distribution in four different states by COMSOL are presented in Figure 2b. Because of its unique working mechanism and excellent outputting voltage characteristics, it can be well used for monitoring various sports items.

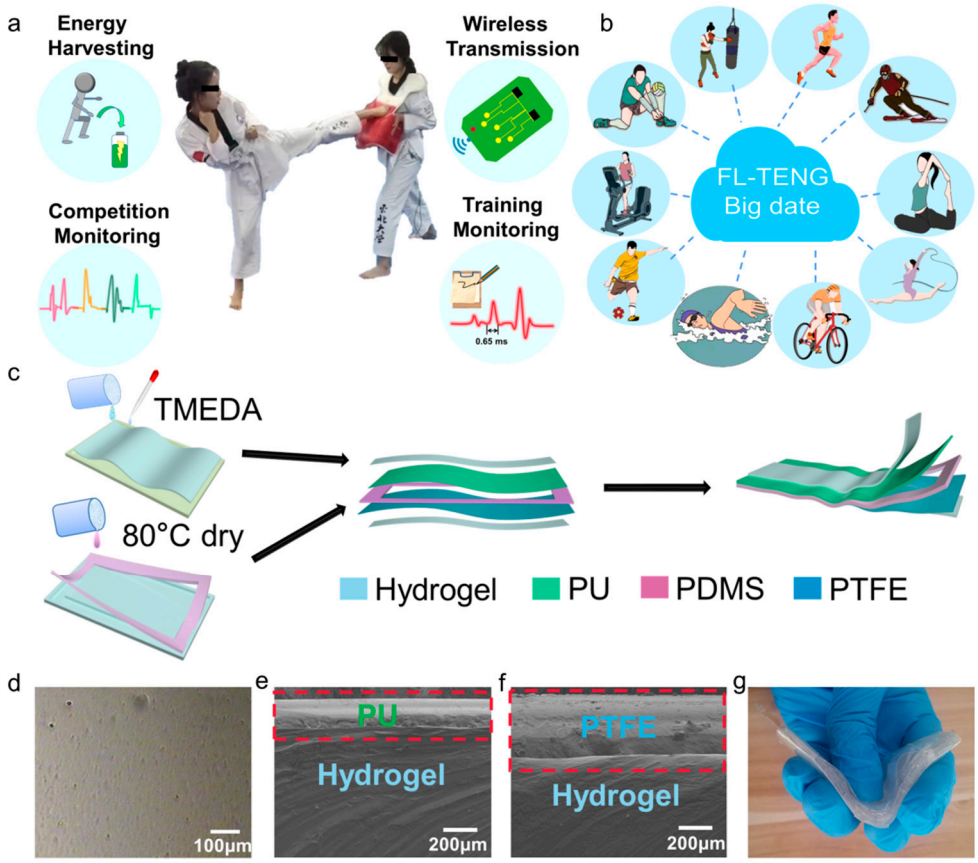

Figure 1. Application and production of FL-TENG. (**a**) Application of FL-TENG in taekwondo competition. (**b**) The sports application scenario of FL-TENG. (**c**) The fabrication process of FL-TENG. (**d**) The optical microscope image of polyurethane film. (**e**) The scanning electron microscope image of PU layer cross-section. (**f**) The scanning electron microscope image of PTFE layer cross-section. (**g**) The bending state of FL-TENG.

As a sensor, it is used for sports competition monitoring, and it is important to ensure the sensitivity and stability of the sensor. Therefore, we tested the electrical output performance of the FL-TENG, as shown in Figure 3. We fixed the FL-TENG with a size of 7.8 × 3 cm and a friction contact area of 6 × 2.5 cm^2 to a stepper motor and we used the stepper motor to imitate the striking process in a taekwondo competition. Figure 3a shows the output voltage of FL-TENG at different bending angles at the same frequency (1 Hz), and the frictional electric output voltage is 23, 38, 56, and 67 V when the bending angles are 3.22°, 4.22°, 5.21°, and 6.21°, respectively. The angle test scenario is shown in Figure S1. Figure 3b shows the linear relationship between the FL-TENG bending angle

and the output voltage. The Pearson correlation coefficient is 0.996, which indicates a significant linear relationship between the angle and voltage. The equation is:

$$V \approx -25 + 15.06 \times \text{degree} \quad (1)$$

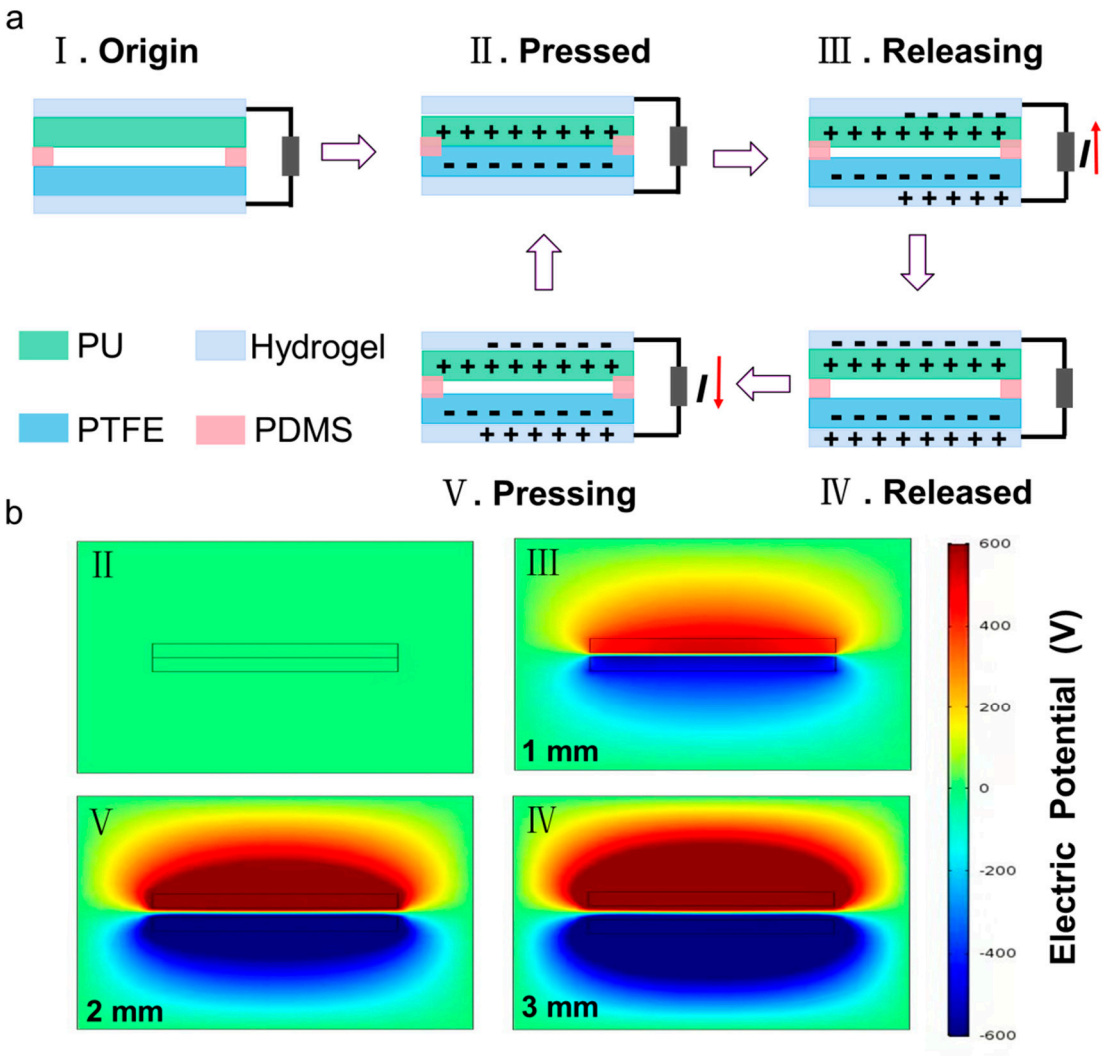

Figure 2. The working mechanism of FL-TENG. (**a**) Schematics of the operating principle for the FL-TENG. (I) The original state of FL-TENG. (II) FL-TENG is compressed. (III) FL-TENG release process. (IV) FL-TENG is released. (V) FL-TENG release process. (**b**) Potential simulations were performed by COMSOL to elucidate the working principle of FL-TENG. (II) FL-TENG compressed potential simulation. (III) FL-TENG release process potential simulation. (IV) FL-TENG is released potential simulation. (V) FL-TENG release process potential simulation.

The output voltage is measured at the same bending angle and different frequencies in Figure 3c. The output voltages are 97 V, 97 V, 97 V, and 97 V when the frequencies are 1 Hz, 2 Hz, 3 Hz, and 4 Hz, respectively. The frequency test scenario is shown in Figure S2. It demonstrates that the output voltage of FL-TENG is very stable. Figure 3d shows the response of the FL-TENG at different frequencies. The response of the FL-TENG is calculated by the following equation:

$$R\% = \left| \frac{V_0 - V_i}{V_i} \right| \times 100\% \quad (2)$$

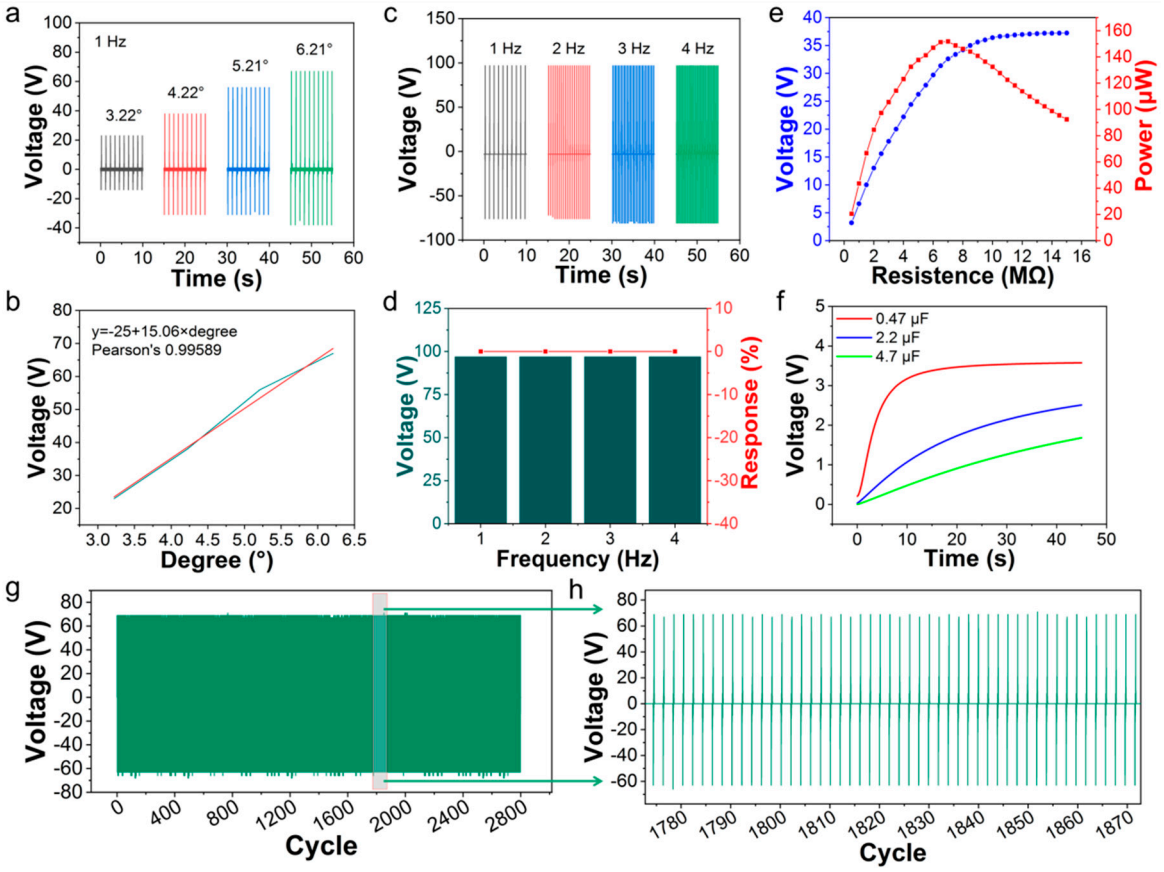

Figure 3. The output performance of FL-TENG. (**a**) The output voltage of FL-TENG at the same frequency with different bending angles. (**b**) The output voltage of FL-TENG at the same frequency with different bending angles, and linear relationship between bending angle and voltage. (**c**) The output voltage of FL-TENG at the same bending angle with different frequencies. (**d**) Voltage and response of FL-TENG at different frequencies. (**e**) Voltage and power of FL-TENG under different load resistances. (**f**) Charging of 0.47 μF, 2.2 μF, and 4.7μF capacitors by FL-TENG. (**g**) Durability test of FL-TENG. (**h**) Details of the durability test.

In which V_0 and V_i are the output voltage when the frequency is 1 Hz and the output voltage when the frequency is another frequency. The response of FL-TENG is 0 when the frequency is 1 Hz, 2 Hz, 3 Hz, and 4 Hz. The data result demonstrates that when the angle change is certain, the change of the frequency does not cause the change of the output voltage, and the output voltage is kept stable. It indicates that the FL-TENG has excellent performance for competition taekwondo referee monitoring, and it can sensitively and monitor the initiative and effectiveness of both players' attacks accurately. For example, in taekwondo competitions, cases often happen that both athletes end up with the same score. In such cases, the winner is usually determined by the referee's subjective judgment, i.e., the side with the stronger offensive initiative wins. However, due to the subjective nature of the situation, the application of FL-TENG can provide a credible basis for referee judging in these situations. Figure 3e shows the output voltage and output power of the FL-TENG with different load resistances. It can be observed that the output voltage increases with the increases of load resistance, and the power of FL-TENG reaches the maximum of 151.8 μW when the load resistance is 7 MΩ; thus, it can be known that the resistance of FL-TENG is 7 MΩ. Figure 3f shows that the FL-TENG charges different capacitors, and when the bending angle and frequency are kept fixed, the FL-TENG charges 0.47 μF, 2.2 μF, and 4.7 μF capacitors for 45 s, which can be charged to 3.6 V, 2.5 V, and 1.7 V. This demonstrates that the FL-TENG can be used as both a sensor and an energy collector to convert the mechanical energy of motion into electrical energy for self-powering. Figure 3g shows the

durability test of the FL-TENG. After 2800 cycles of testing, the FL-TENG still maintains a stable output, and Figure 3h shows the details of the durability test, which demonstrates that the device has a long working stability and ensures the accuracy of sense; it saves time for debugging the device in taekwondo competitions.

In the electrode selection, the hydrogel has good stretchable and conductive properties to meet our needs for a practical application in taekwondo competitions, and the hydrogel is not easily broken compared with a steel electrode, which ensures the stability of FL-TENG sensing and the lifetime of the sensor device. To verify whether hydrogel electrodes have an impact on the electrical output of the sensor device, we used hydrogel electrodes and copper electrodes for a comparative test. Figure 4a shows the device output voltage of hydrogel electrodes at the same frequency and bending angle. The output voltage is 87 V. The 40 green LEDs light up easily (Video S1). Figure 4b shows the device output voltage of the copper thin film electrode at the same frequency and bending angle. The output voltage is 102 V and it can also light up to 40 green LEDs (Video S1). Hydrogel electrodes and copper electrodes can achieve the same effect. However, the hydrogel electrode has good stretchable properties; therefore, it is the best choice to use hydrogel in this study. The range of voltage output of the FL-TENG is measured. A spitball is dropped on the surface of the FL-TENG and we smash the device directly with a fist (Figure 4c). The output voltage is 0.8 V and 514 V, respectively. The result indicated that the FL-TENG has good sensitivity properties. Figure 4d shows the wireless Bluetooth transmission system. The FL-TENG sensor is linked to the Bluetooth signal transmitter module, and when there is no sensing signal, the Bluetooth signal receiving module illuminates one LED. As shown in Figure 4d(I), when the taekwondo player makes an effective strike, the signal produced by the device is sent by the Bluetooth transmitter module, and three lights illuminate when the signal is received by the Bluetooth receiver module, as shown in Figure 4d(II). In Video S2, it can be observed that the frequency of the Bluetooth signal receiving module lights up is controlled by FL-TENG. This simple and mature wireless signal transmission technology opens up a wide range of applications for FL-TENG in sports monitoring.

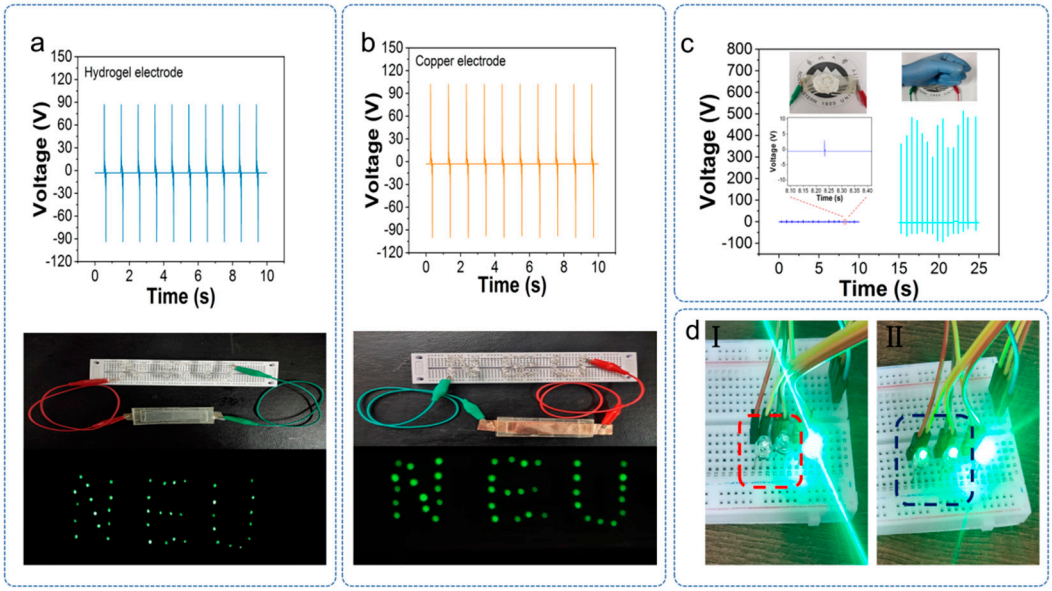

Figure 4. Output performance, sensitivity and wireless sensing tests of the hydrogel electrode FL-TENG. (**a**) Hydrogel electrode output voltage and lighting of 40 green LEDs. (**b**) Output voltage of copper electrode and lighting of 40 green LEDs. (**c**) Sensitivity test of FL-TENG. (**d**) Wireless Bluetooth transmission test. (I) LED lights are not lit up. (II) LED lights are lit up.

Competitive taekwondo is a high spectator sport in which athletes use their legs for offense and defense; it requires athletes to score points by using practical and effective skills

to strike the opponent's torso or head in a fierce confrontation. The final score is influenced by two main factors: one is the athletes' ability to compete in taekwondo, the other are the judges' decisions. Figure 5a shows a male taekwondo athlete performance with a light power kick, a medium power kick, and a heavy power kick by the turning kick technique (Video S3). The average voltage is obtained from five kicks of light, medium, and heavy power. The output voltage is 128.4 V, 149.6 V, and 197.6 V, respectively. The smoothness of the three phases of overload indicates that the male athlete has good control in the power of the leg and he can quickly change the rhythm of attack in taekwondo competitions. Figure 5b shows the female taekwondo athlete performance with light power kicks, medium power kicks, and heavy power kicks by the turning kick technique (Video S4). The average voltage values are obtained from five kicks with light, medium, and heavy power, and the output voltage are 45.5 V, 137.8 V, and 152.2 V. The result demonstrates that the female athlete has too much span from light to medium power kicks and she has poor control in the leg power. The turning kick is a frequently used action in taekwondo competition, and the kick attack of moderate strength plays an important role in adjusting the attack rhythm in the taekwondo turning kick technique; however, it is also the most difficult technical action to master, and it is difficult for coaches to monitor it in training. Figure 5a,b shows that FL-TENG enables the monitoring of light to medium to heavy overload of power in the turning kick technique and assists coaches in implementing targeted training. Table 1 shows the detailed data of the athletes' medium-strength turning kicks. The average time for each hit and the standard variance of the hit times for both male and female athletes demonstrate that the male athletes completed the movement faster and more consistently, which further proves that the male athletes have better control of their leg muscle strength. In addition, the average voltage of each hit and the standard variance of output voltage were both higher for males than for females, which implies that male athletes have better strength and rhythm change than female athletes. In taekwondo competition rules, it is stipulated that the effective area for the scoring offense is below the clavicle, above the hip bone, both sides of the rib, and the protective part of the head guard. The athlete strikes the opponent's back, resulting in a warning or even a penalty. In the taekwondo competition, a 360° turning kick is the most ornamental technical action, but the large amplitude and fast speed of this technical action leads to low striking accuracy. To score effectively, it requires the athlete to precisely strike the effective scoring area of the guard. Figure 5c shows a male athlete kicking a taekwondo guard with the 360° turning kick technique (Video S5). Out of security concerns, we used a stationary guard as a target and kicked the front of the guard. The output voltage is 138 V, 156 V, 194 V, 130 V, and 16 V of the five 360° kicks, and the Video S5 demonstrates that the fifth kick lost accuracy and resulted in a low output voltage. It also solves the problem when the referee hears the sound and gives the score (sometimes the referee does not see the hitting position but hears the sound due to the obstructed vision). Figure 5d shows the voltage output of the female athlete kicking the taekwondo guard five times with the 360° turning kick technique, the five output voltages are 84 V, 167 V, 167 V, 132 V, and 149 V. In this actual test, to ensure the accuracy of the strikes, we asked the athlete to use a decomposed slow motion in the test (Video S6). The results of the FL-TENG test demonstrate that the accuracy of the strikes improve when the amplitude and speed of the movements reduce. Although it is not possible to slow down the movement speed in formal competition, it can be applied in training, because the formation of motor skills goes through the stages of generalization, differentiation, consolidation, and automation. The decomposition of slow movements is equivalent to the differentiation stage of skill formation, which is characterized by a coherent technical movement and the initial formation of power stereotypes. The second and third voltage in Figure 5d are visual reflections of the power stereotypes of the motor skill. The unification of speed and precision is achieved through continuous training after power stereotypes. The monitoring data in Figure 5d illustrates that FL-TENG can also be applied to the monitoring in various stages of motor skill formation. In an intense taekwondo match, quick and effective technical movements are the key to scoring points. Figure 5e shows the

output voltage generated by the female athlete by back kick, side kick, and turning kick techniques (Video S7). From the three sets of voltage magnitudes, it can be observed that the athlete strikes the best with the turning kick technique (Video S7); this demonstrates that the athlete mastered the most proficient turning kick technique, where the third attack of the back kick technique has not produced an effective hit. From the Figure 5e and Video S7, the foot and the guard are in contact. In a real competition, the referee judges it as a valid attack and scores a point, and then there is a dispute, whichaffects the normal competition. The FL-TENG can be used as a judging system, which makes the competition fairer. Meanwhile, the FL-TENG can also contribute to the data of the athletes' mastering proficiency in various techniques, which helps coaches to make reasonable tactics.

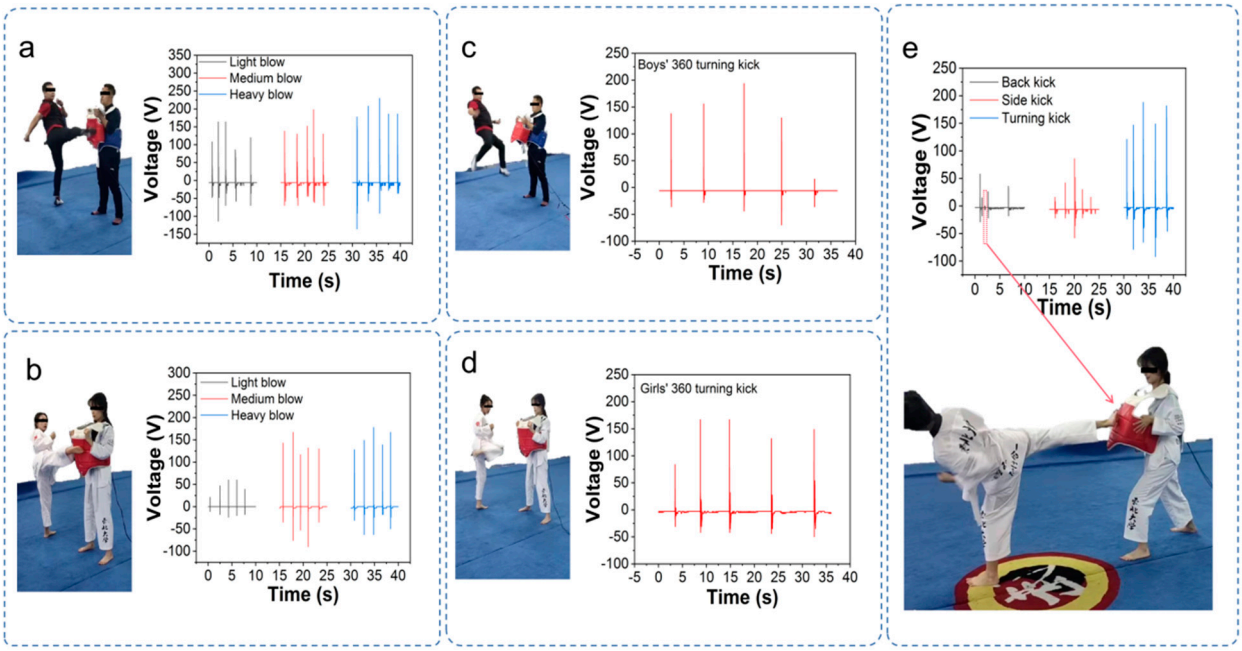

Figure 5. Actual test of FL-TENG. (**a**) Turning kick test for male athletes. (**b**) Turning kick test for female athletes. (**c**) Male athlete 360° turning kick test. (**d**) Female athlete 360° turning kick test. (**e**) Back kick, side kick, and turning kick proficiency test for female athletes.

Table 1. Athletes' medium-strength turning kick data.

	Male Athletes	Female Athletes
Total number of hits	5	5
Average time of each hit	0.049 s	0.127 s
Standard variance of hit times	0.004	0.026
Average voltage of each hit	149.6 V	137.8 V
Standard variance of output voltage	25.50	17.28

In addition, the FL-TENG can distinguish between scoring actions and unsportsmanlike actions to assist the referee in making better real-time judgments. Combined with the excellent output performance of FL-TENG, we use it to build an unsportsmanlike action monitoring system. The circuit of this monitoring system is illustrated in Supplementary Figure S1. The unsportsmanlike action is synchronously collected and transmitted wirelessly through the transmitter side of the system to the receiver side, which is connected to a computer, through which the validity of the action is judged in real time (Figure 6a). We demonstrate the feasibility of our device with a simple tapping experiment (Video S8). Figure 6b shows the output voltage and detail plots for the punch action (the only hand action allowed), and the unsportsmanlike penalty scoring action, which includes elbow blows, knee bumps, and palm pushes, produces the output voltage and detail plots shown

in Figure 6c–e. The results demonstrate that different body parts attacked by the virus will produce different voltage waveforms. In the punch movement, there is an internal rotation in the fist. The face of the punch produces complex force transmission. Therefore, it produces complex multiple waveforms in Figure 6b(ii), elbow blows produce regular single waveforms in Figure 6c(ii), knee bumps produce regular double waveforms in Figure 6d(ii), and palm pushes produce a time delay between the upper and lower waveforms in Figure 6e(ii). The combination of FL-TENG and the monitoring system provides more convenience for taekwondo competition monitoring.

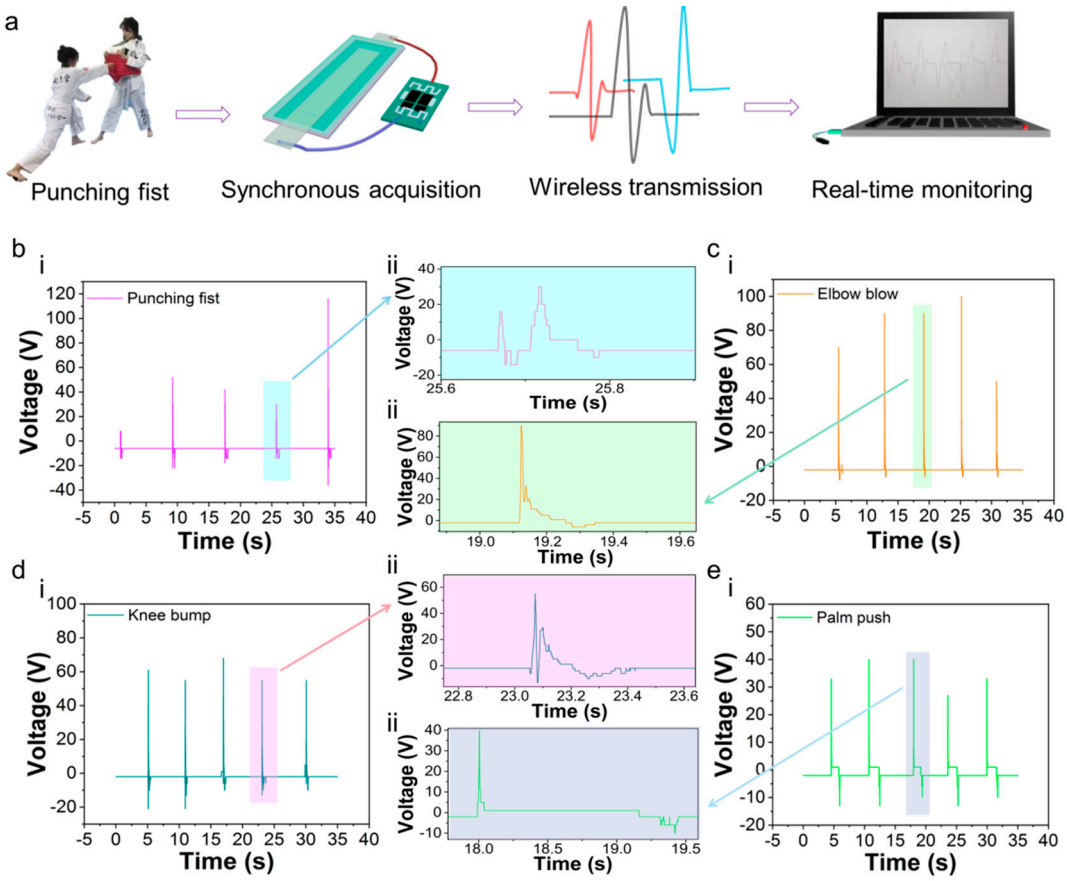

Figure 6. FL-TENG monitoring foul action and monitoring system. (**a**) Unsportsmanlike action monitoring system. (**b**) Voltage and waveform generated by punching. (i) The punching fist voltage graphs. (ii) The detail graphs of punching fist voltage. (**c**) Voltage and waveform generated by elbow blow. (i) The elbow blow voltage graphs. (ii) The detail graphs of elbow blow voltage. (**d**) Voltage and waveform generated by knee bump. (i) The knee bump voltage graphs. (ii) The detail graphs of knee bump voltage. (**e**) Voltage and waveform generated by palm push. (i) The palm push voltage graphs. (ii) The detail graphs of palm push voltage.

4. Conclusions

In summary, we have fabricated a flexible and lightweight triboelectric nanogenerator that uses polytetrafluoroethylene (PTFE) and polyurethane (PU) membranes as frictional layers and hydrogels as electrodes. FL-TENG achieves the sensitive monitoring of the bending angle and frequency changes by using a contact separation mode, and FL-TENG is able to convert the biomechanical energy of motion into electrical energy while achieving sensing and self-power. We use FL-TENG in taekwondo competition monitoring to improve the fairness and impartiality of the judges. At the same time, FL-TENG is combined with a wireless monitoring system to realize the real-time presentation of monitoring data, which provides more paths for digitalization and intelligence in sports competitions.

Supplementary Materials: The following supporting information can be downloaded at: https://www.mdpi.com/article/10.3390/electronics11091306/s1, Figure S1. The angle test scenario photographs. Figure S2. The frequency test scenario photographs. Figure S3: The circuit of unsportsmanlike action monitoring system. Video S1: Test of dot LED lamp for hydrogel electrode device and copper electrode device. Video S2: Wireless Bluetooth transmission system. Video S3: Turning kick test for male athletes. Video S4: Turning kick test for female athletes. Video S5: Male athlete 360° turning kick test. Video S6: Female athlete 360° turning kick test. Video S7: Back kick, side kick, and turning kick proficiency test for female athletes. Video S8: Test of unsportsmanlike action monitoring system.

Author Contributions: Data curation, formal analysis, and writing—original draft, software, and investigation, F.S.; data curation, formal analysis, visualization, and investigation, Y.Z. and C.J.; investigation and visualization, B.O.; formal analysis visualization, T.Z.; software and visualization, C.L.; conceptualization, N.B.; conceptualization, X.L.; supervision, resources, and writing—review and editing, S.C.; conceptualization, resources, and writing—review and editing, T.C.; conceptualization supervision, resources, and writing—review and editing, Y.M. All authors have read and agreed to the published version of the manuscript.

Funding: This research did not receive any specific grant from funding agencies in the public, commercial, or not-for-profit sectors.

Informed Consent Statement: Informed consent was obtained from all subjects involved in the study.

Acknowledgments: We thank Xiang Wu at Shenyang University of Technology and Ning Ba at Tsinghua University for their helpful discussion.

Conflicts of Interest: The authors declare no conflict of interest.

References

1. Bistron, M.; Piotrowski, Z. Artificial Intelligence Applications in Military Systems and Their Influence on Sense of Security of Citizens. *Electronics* **2021**, *10*, 871. [CrossRef]
2. Lv, Z.H.; Song, H.B.; Basanta-Val, P.; Steed, A.; Jo, M. Next-Generation Big Data Analytics: State of the Art, Challenges, and Future Research Topics. *IEEE Trans. Industr. Inform.* **2017**, *13*, 1891–1899. [CrossRef]
3. Gams, M.; Kolenik, T. Relations between Electronics, Artificial Intelligence and Information Society through Information Society Rules. *Electronics* **2021**, *10*, 514. [CrossRef]
4. Khorsand, M.; Tavakoli, J.; Guan, H.W.; Tang, Y.H. Artificial intelligence enhanced mathematical modeling on rotary triboelectric nanogenerators under various kinematic and geometric conditions. *Nano Energy* **2020**, *75*, 104993. [CrossRef]
5. Zhou, Y.K.; Shen, M.L.; Cui, X.; Shao, Y.C.; Li, L.J.; Zhang, Y. Triboelectric nanogenerator based self-powered sensor for artificial intelligence. *Nano Energy* **2021**, *84*, 105887. [CrossRef]
6. Yun, J.; Jayababu, N.; Kim, D. Self-powered transparent and flexible touchpad based on triboelectricity towards artificial intelligence. *Nano Energy* **2020**, *78*, 105325. [CrossRef]
7. Guan, H.; Zhong, T.; He, H.; Zhao, T.; Xing, L.; Zhang, Y.; Xue, X. A self-powered wearable sweat-evaporation-biosensing analyzer for building sports big data. *Nano Energy* **2019**, *59*, 754–761. [CrossRef]
8. Naugler, C.; Church, D.L. Automation and artificial intelligence in the clinical laboratory. *Crit. Rev. Clin. Lab Sci.* **2019**, *56*, 98–110. [CrossRef]
9. Dahmen, J.; Thomas, B.L.; Cook, D.J.; Wang, X. Activity Learning as a Foundation for Security Monitoring in Smart Homes. *Sensors* **2017**, *17*, 737. [CrossRef]
10. Kang, W.M.; Moon, S.Y.; Park, J.H. An enhanced security framework for home appliances in smart home. *Hum.-Cent. Comput. Inf. Sci.* **2017**, *7*, 6. [CrossRef]
11. Shin, J.; Park, Y.; Lee, D. Who will be smart home users? An analysis of adoption and diffusion of smart homes. *Technol. Forecast Soc. Change* **2018**, *134*, 246–253. [CrossRef]
12. Yu, L.; Kong, D.; Shao, X.; Yan, X. A Path Planning and Navigation Control System Design for Driverless Electric Bus. *IEEE Access* **2018**, *6*, 53960–53975. [CrossRef]
13. Hsu, T.-Y.; Nieh, C.P. On-Site Earthquake Early Warning Using Smartphones. *Sensors* **2020**, *20*, 2928. [CrossRef]
14. Kuyuk, H.S.; Colombelli, S.; Zollo, A.; Allen, R.M.; Erdik, M.O. Automatic earthquake confirmation for early warning system. *Geophys. Res. Lett.* **2015**, *42*, 5266–5273. [CrossRef]
15. Baldauf, R.; Watkins, N.; Heist, D.; Bailey, C.; Rowley, P.; Shores, R. Near-road air quality monitoring: Factors affecting network design and interpretation of data. *Air Qual. Atmos. Health* **2009**, *2*, 1–9. [CrossRef]
16. Noriega-Linares, J.E.; Ruiz, J.M.N. On the Application of the Raspberry Pi as an Advanced Acoustic Sensor Network for Noise Monitoring. *Electronics* **2016**, *5*, 74. [CrossRef]
17. Kang, J.; Hwang, K.-I. A Comprehensive Real-Time Indoor Air-Quality Level Indicator. *Sustainability* **2016**, *8*, 881. [CrossRef]

18. Persaud, K.C.; Wareham, P.; Pisanelli, A.M.; Scorsone, E. "Electronic nose"—New condition monitoring devices for environmental applications. *Chem. Senses* **2005**, *30*, i252–i253. [CrossRef]
19. Chang, B. Application of Heart Rate Acceleration Motion Wireless Sensor Fusion in Individual Special Competitive Sports. *J Sens.* **2021**, *2021*, 5723567. [CrossRef]
20. Taffoni, F.; Rivera, D.; La Camera, A.; Nicolo, A.; Ramon Velasco, J.; Massaroni, C. A Wearable System for Real-Time Continuous Monitoring of Physical Activity. *J. Healthc. Eng.* **2018**, *2018*, 1878354. [CrossRef]
21. Li, J.; Long, Y.; Yang, F.; Wei, H.; Zhang, Z.; Wang, Y.; Wang, J.; Li, C.; Carlos, C.; Dong, Y.; et al. Multifunctional Artificial Artery from Direct 3D Printing with Built-In Ferroelectricity and Tissue-Matching Modulus for Real-Time Sensing and Occlusion Monitoring. *Adv. Funct. Mater.* **2020**, *30*, 2002868. [CrossRef] [PubMed]
22. Lin, B.-S.; Lin, B.-S.; Chou, N.-K.; Chong, F.-C.; Chen, S.-J. RTWPMS: A real-time wireless physiological monitoring system. *IEEE Trans. Inf. Technol. Biomed.* **2006**, *10*, 647–656. [CrossRef]
23. Fung, J. Gait and balance training using virtual reality is more effective for improving gait and balance ability after stroke than conventional training without virtual reality. *J. Physiother.* **2017**, *63*, 114. [CrossRef] [PubMed]
24. Chi, E.H. Introducing wearable force sensor's in martial arts. *IEEE Pervas. Comput.* **2005**, *4*, 47–53. [CrossRef]
25. Li, L.; Liu, W.-D.; Liu, Q.; Chen, Z.-G. Multifunctional Wearable Thermoelectrics for Personal Thermal Management. *Adv. Funct. Mater.* **2022**, 2200548. [CrossRef]
26. Chen, Z.-G.; Liu, W.-D. Thermoelectric coolers: Infinite potentials for finite localized microchip cooling. *J. Mater. Sci. Technol.* **2022**, *121*, 256–262. [CrossRef]
27. Chen, Z.-G.; Shi, X.; Zhao, L.-D.; Zou, J. High-performance SnSe thermoelectric materials: Progress and future challenge. *Prog. Mater. Sci.* **2018**, *97*, 283–346. [CrossRef]
28. Fan, F.-R.; Tian, Z.-Q.; Wang, Z.L. Flexible triboelectric generator! *Nano Energy* **2012**, *1*, 328–334. [CrossRef]
29. Ahmed, A.; Hassan, I.; Hedaya, M.; El-Yazid, T.A.; Zu, J.; Wang, Z.L. Farms of triboelectric nanogenerators for harvesting wind energy: A potential approach towards green energy. *Nano Energy* **2017**, *36*, 21–29. [CrossRef]
30. Zhou, Q.; Lee, K.; Deng, S.; Seo, S.; Xia, F.; Kim, T. Portable triboelectric microfluidic system for self-powered sensors towards in-situ detection. *Nano Energy* **2021**, *85*, 105980. [CrossRef]
31. Jiang, T.; Yao, Y.; Xu, L.; Zhang, L.; Xiao, T.; Wang, Z.L. Spring-assisted triboelectric nanogenerator for efficiently harvesting water wave energy. *Nano Energy* **2017**, *31*, 560–567. [CrossRef]
32. Lee, S.; Lee, Y.; Kim, D.; Yang, Y.; Lin, L.; Lin, Z.-H.; Hwang, W.; Wang, Z.L. Triboelectric nanogenerator for harvesting pendulum oscillation energy. *Nano Energy* **2013**, *2*, 1113–1120. [CrossRef]
33. Seol, M.-L.; Woo, J.-H.; Jeon, S.-B.; Kim, D.; Park, S.-J.; Hur, J.; Choi, Y.-K. Vertically stacked thin triboelectric nanogenerator for wind energy harvesting. *Nano Energy* **2015**, *14*, 201–208. [CrossRef]
34. Wang, Z.L.; Jiang, T.; Xu, L. Toward the blue energy dream by triboelectric nanogenerator networks. *Nano Energy* **2017**, *39*, 9–23. [CrossRef]
35. Zou, Y.; Raveendran, V.; Chen, J. Wearable triboelectric nanogenerators for biomechanical energy harvesting. *Nano Energy* **2020**, *77*, 105303. [CrossRef]
36. Ma, Y.; Ouyang, J.; Raza, T.; Li, P.; Jian, A.; Li, Z.; Liu, H.; Chen, M.; Zhang, X.; Qu, L.; et al. Flexible all-textile dual tactile-tension sensors for monitoring athletic motion during taekwondo. *Nano Energy* **2021**, *85*, 105941. [CrossRef]
37. Mao, Y.; Zhu, Y.; Zhao, T.; Jia, C.; Bian, M.; Li, X.; Liu, Y.; Liu, B. A Portable and Flexible Self-Powered Multifunctional Sensor for Real-Time Monitoring in Swimming. *Biosensors* **2021**, *11*, 147. [CrossRef]
38. Zhu, Y.; Sun, F.; Jia, C.; Zhao, T.; Mao, Y. A Stretchable and Self-Healing Hybrid Nano-Generator for Human Motion Monitoring. *Nanomaterials* **2022**, *12*, 104. [CrossRef]
39. Jia, C.; Zhu, Y.; Sun, F.; Zhao, T.; Xing, R.; Mao, Y.; Zhao, C. A Flexible and Stretchable Self-Powered Nanogenerator in Basketball Passing Technology Monitoring. *Electronics* **2021**, *10*, 2584. [CrossRef]
40. Zhou, Q.; Lee, K.; Kim, K.N.; Park, J.G.; Pan, J.; Bae, J.; Baik, J.M.; Kim, T. High humidity-and contamination-resistant triboelectric nanogenerator with superhydrophobic interface. *Nano Energy* **2019**, *57*, 903–910. [CrossRef]
41. Pu, X.; An, S.; Tang, Q.; Guo, H.; Hu, C. Wearable triboelectric sensors for biomedical monitoring and human-machine interface. *Iscience* **2021**, *24*, 102027. [CrossRef] [PubMed]
42. Xu, Q.; Fang, Y.; Jing, B.Q.; Hu, N.; Lin, K.; Pan, Y.; Xu, L.; Gao, H.; Yuan, M.; Chu, L.; et al. A portable triboelectric spirometer for wireless pulmonary function monitoring. *Biosens. Bioelectron.* **2021**, *187*, 113329. [CrossRef] [PubMed]
43. Zhao, T.; Fu, Y.; He, H.; Dong, C.; Zhang, L.; Zeng, H.; Xing, L.; Xue, X. Self-powered gustation electronic skin for mimicking taste buds based on piezoelectric-enzymatic reaction coupling process. *Nanotechnology* **2018**, *29*, 075501. [CrossRef] [PubMed]
44. Zhao, Y.; He, J.F.; Dai, M.Z.; Zhao, D.P.; Wu, X.; Liu, B.D. Emerging CoMn-LDH@MnO2 electrode materials assembled using nanosheets for flexible and foldable energy storage devices. *J. Energy Chem.* **2020**, *45*, 67–73. [CrossRef]
45. Cheng, P.; Guo, H.; Wen, Z.; Zhang, C.; Yin, X.; Li, X.; Liu, D.; Song, W.; Sun, X.; Wang, J.; et al. Largely enhanced triboelectric nanogenerator for efficient harvesting of water wave energy by soft contacted structure. *Nano Energy* **2019**, *57*, 432–439. [CrossRef]
46. Luo, J.; Wang, Z.; Xu, L.; Wang, A.C.; Han, K.; Jiang, T.; Lai, Q.; Bai, Y.; Tang, W.; Fan, F.R.; et al. Flexible and durable wood-based triboelectric nanogenerators for self-powered sensing in athletic big data analytics. *Nat. Commun.* **2019**, *10*, 5147. [CrossRef] [PubMed]

47. Lu, Q.; Chen, H.; Zeng, Y.; Xue, J.; Cao, X.; Wang, N.; Wang, Z. Intelligent facemask based on triboelectric nanogenerator for respiratory monitoring. *Nano Energy* **2022**, *91*, 106612. [CrossRef]
48. Garcia, C.; Trendafilova, I.; de Villoria, R.G.; del Rio, J.S. Self-powered pressure sensor based on the triboelectric effect and its analysis using dynamic mechanical analysis. *Nano Energy* **2018**, *50*, 401–409. [CrossRef]